

Manuscript received May 18, 2022; revised August 20, 2022; accepted August 12, 2022; date of publication August 25, 2022

Digital Object Identifier (DOI): <https://doi.org/10.35882/ijahst.v2i4.239>

Copyright © 2022 by the authors. This work is an open-access article and licensed under a Creative Commons Attribution-ShareAlike 4.0 International License ([CC BY-SA 4.0](https://creativecommons.org/licenses/by-sa/4.0/))

How to cite: M. Bagus F. I, Moch Prastawa ATP, SY Setiawan, Lamidi, IDG Hariwisana, TB Indrato, "Effect of Muscle Fatigue on Heart Signal on Physical Activity with Electromyogram and Electrocardiogram Monitoring Signals", Indonesian Journal of Electronics, Electromedical Engineering, and Medical Informatics, vol. 4, no. 3, pp. 138–144, Augustus. 2022.

Utilization of High-Power LEDs at Low-Cost Non-Invasive X-ray KV Meter Detectors Design

M. Bagus F. I, Moch Prastawa A T P, S Y Setiawan, Lamidi, I D G Hariwisana, T B Indrato, and Mansour Asghari

¹ Department of Medical Electronics Technology, Poltekkes Kemenkes Surabaya, Indonesia

² Bonab Islamic Azad university, Bonab, Iran

Corresponding author: Moch Prastawa ATP (email: prast77@poltekkesdepkes-sby.ac.id)

ABSTRACT X-ray radiation is used to diagnose human body. In order to apply this method, two parameters are commonly used as the settings. The first is the KV value and the second is the mA value. In this case, when an error occurs in the kV setting, it will cause poor image quality, thus leads to inaccurate information in patient's examination. It is likewise the presence of excessive doses to the patient's body. To ensure that the KV value produced is under the settings on the machine consul, both invasive and non-invasive measurements were carried out. Non-invasive is becoming an easy standard to do. Several types of equipment on the market and research results have been widely used for this non-invasive activity. The problem emerges is that the existing tools still use expensive detectors. The purpose of this study was to design a low-cost non-invasive x-ray KV meter detector using an LED detector whose ability was tested at each point of collimation. Furthermore, the method used in this study was to stump the detectors at 4 ends of the collimation by 20 cm apart. The data were taken by doing x-ray exposure at a distance of 60 cm. The module measurements were carried out under 80 mA exposure conditions for 1 second and a collimation area of 20 x 20 cm. Meanwhile, the x-ray exposure settings were performed at 40kV, 50kV, 60kV, and 70kV settings. The module measurement results were further compared to the x-ray machine setting values. Based on the comparison results, the smallest error rate was obtained on Sensor 2 by 0.83%, while the highest error rate was obtained on S5 by 6.43%. The results can be concluded that the LED phosphor can capture x-rays, but the detector was weak due to the interference from ambient light. In addition, the results obtained from the detector itself were still less stable and linear. Furthermore, the implications of the results of this study are the initial basis for the use of high-power LEDs as sensors in non-invasive X-ray KV factor detection. In future research, stability and linearity should be built using a mechanical design that is able to reduce the ambient light interference.

INDEX TERMS High Power LED, X-Ray, Radiation, Non-Invasive KV Meter

I. Introduction

Radiology has become an important part of modern medicine, particularly one of the most powerful and important diagnostic tools today. It is estimated that around 30% to 50% of important medical decisions are based on x-rays. As an example, radiologists from the Norwegian Medical Association were required to evaluate potential reasons for increased irradiation and unnecessary irradiation (15 cases) in a questionnaire. The results showed that the greatest increase in the use of radiology is due to the new radiation technologies, human needs, the uncertainty of physician diagnosis, as well as the increase and availability of clinical indications [1]–[4]. X-ray is a type of electromagnetic energy that is very useful in medical fields including for disease diagnosis and health care. Furthermore, x-ray machines of both radiography and fluoroscopy are also often used to determine the condition of human body. To use this machine, two parameters are commonly used for the settings [5][6]. The first parameter is the KV value, while the second parameter is the mA value. In this case,

incorrect voltage and current regulation in operating the systems for diagnostic and therapeutic purposes can harm body tissue systems and provide inaccurate patient information. Apart from human error, errors can also occur when X-ray equipment starts to fail or becomes unusable [7], [8]. Therefore, it is necessary to check the settings of these important parameters before using the X-ray equipment [9][10]. Therefore, in order to maintain and receive accurate information about the performance of the X-ray machine, a high accuracy and precision must be calibrated [11]. In the non-invasive method, x-ray tube tension measurements are carried out without direct contact. This measurement uses the conversion of the value of the radiation emitted by the x-ray machine and is measured using a radiation meter that is placed according to the standard [12][13]. In this case, two systems are used. The first system is an ion sensor that directly converts x-ray radiation into an electric current. Meanwhile, the second system is converting the x-rays into visible light whose intensity is further measured. The measurement process begins with the conversion of X-

rays into visible light using a scintillator. The amount of light is further converted into several voltages by the photomultiplier tube. In addition, the ADC also converts analog data to digital data to be displayed on a PC [14]–[16]. In this case, Monte Carlo method is a useful and powerful tool for simulating the Compton scattering technique to obtain X-ray spectra. The point source model is useful to get a good approximation of the process. In addition, geometric spectrometers can simplify the replacement of shielding and scattering space through narrow solid-angle emission. For this source model, the assembled spectrometer can be drastically simplified without markedly decreasing the accuracy. The full mare model gives not-so-good results, which can further attribute to the fact that the more complicated models, the less it will work well with the small solid angles used for the point source model. Therefore, it is necessary to carry out several experimental measurements to validate the model developed [6], [17]–[20]. Previous research has been carried out on non-invasive x-ray tube voltage measurement. This research used solar cells as the light sensors. In this case, the X-ray employed was captured and illuminated by a fluorescent screen into visible light, which further converted into voltage by the solar cells. Furthermore, this voltage was converted into Kvolt values during the data processing. The drawback of this study is the sensitivity of solar cells to visible light which greatly affected the capabilities of this detector. In addition, fluorescent screens also greatly affected the capabilities of the detector [21]–[23]. In another study entitled PMT (Effect of High Voltage Variations in Solar Tubes) on the Output Amplitude of the NaI (T1) detector, a tool to measure photon radiation has been made using a two-channel analyzer (MCA). The results showed that there was a linear correlation between high voltage and amplitude changes, so reducing the high voltage interval will cause changes in amplitude [24]–[28]. A similar study entitled investigating factors affecting the quality assurance of x-ray surface radiation therapy machines was further done as well. This study also aimed to identify the factors that affected the quality assurance of surface x-ray equipment at Alqura University UMM. In this case, the ionization chamber was used as a sensor. This test was done at 50 kV, 60 mAs, 5 mA, and 0.2 min. The methods used for dosimetry were reproducibility and linearity, while precision was used to measure KV values and exposure time. This research has shown that the quality control of the surface X-ray device indicated that the physical parameters of this device are adequate [10], [12], [13]. Most of the electrons that fall on the target lose their kinetic energy gradually through various collisions, where the energy turns into heat. However, a small number of electrons lose most of their energy and this energy is transformed into X-rays. In this case, the formula obtained is as follows [29]–[32]:

$$Ve = hv_{maks} = \frac{hc}{\lambda_{min}} \quad (1)$$

$$\lambda_{min} = \frac{hc}{Ve} = \frac{1,24 \times 10^{-6} V.m}{v} \quad (2)$$

When the electric quantity is sensitive to the emission of X-ray photons, the LED also acts as a semiconductor detector such as a photodiode. LEDs have a direct energy band gap, while photodiodes have an indirect band gap. In this report, both 34 bpw PD and cool white LEDs are called converters in the sense that they convert energy from one form (photons) to another form (current). This is where the radiation-generated output signal is collected when the PD bpw34 and the white LED chip are exposed to the same diagnostic X-ray. Next, we further explored the possible application of this transducer as a diagnostic X-ray dosimeter. Based on our previous research, cold white LED strips have shown good dosimetric potential when tested on diagnostic x-rays [33]. The use of LEDs could be one of the greatest advances in medical equipment in decades, and LEDs have the advantage of being able to adjust the composition of the resulting spectrum [34]. Another advantage of LEDs is its widespread use of high-intensity and energy-efficient LEDs. The way LEDs work to produce light is by converting electrical energy into light energy. In this mode of operation, LED lamps can immediately emit maximum light, require no warm-up time like light bulbs, and not generate heat like light bulbs and fluorescent lamps. In other studies, the characteristics of LEDs were also used in solar cell research, as a source, and as a detector. In the initial experiment, an electric current was generated when the LED was stimulated by light. The surface of the high-power LED used in the experiment, had a yellow phosphor layer, which functions as a light emitter. As is known that the phosphor coating will also convert X-rays into visible light. Based on the reference above, we can conclude several problems emerged. The first problem is the non-invasive kV detector design which uses a lot of expensive sensors. The next problem is the use of a high-power LED as a light sensor which is still not widely used. In this case, the problem that has not been solved is the high cost of components to make x-ray detectors and the ability of high-power LEDs coated with phosphors which have the potential to become x-ray detectors. Furthermore, the purpose of this study was to utilize high-power LED at a low-cost non-invasive x-ray KV meter detector design and test the ability of the detector at each point of collimation.

II. Materials and Methods

This research was conducted through experimental research. In this case, the author proposed an x-ray selector to be compared with the tool detector. Furthermore, the materials and methods are explained in the following sections.

A. Material

This study designed a non-invasive low-cost KV detector using high-power LEDs that have a phosphor coating. The LEDs used were LEDs on the market. In this case, four LEDs were placed at each measurement point. The measurement point is the point of the outermost corner of the collimation area, so there are 4 measurement

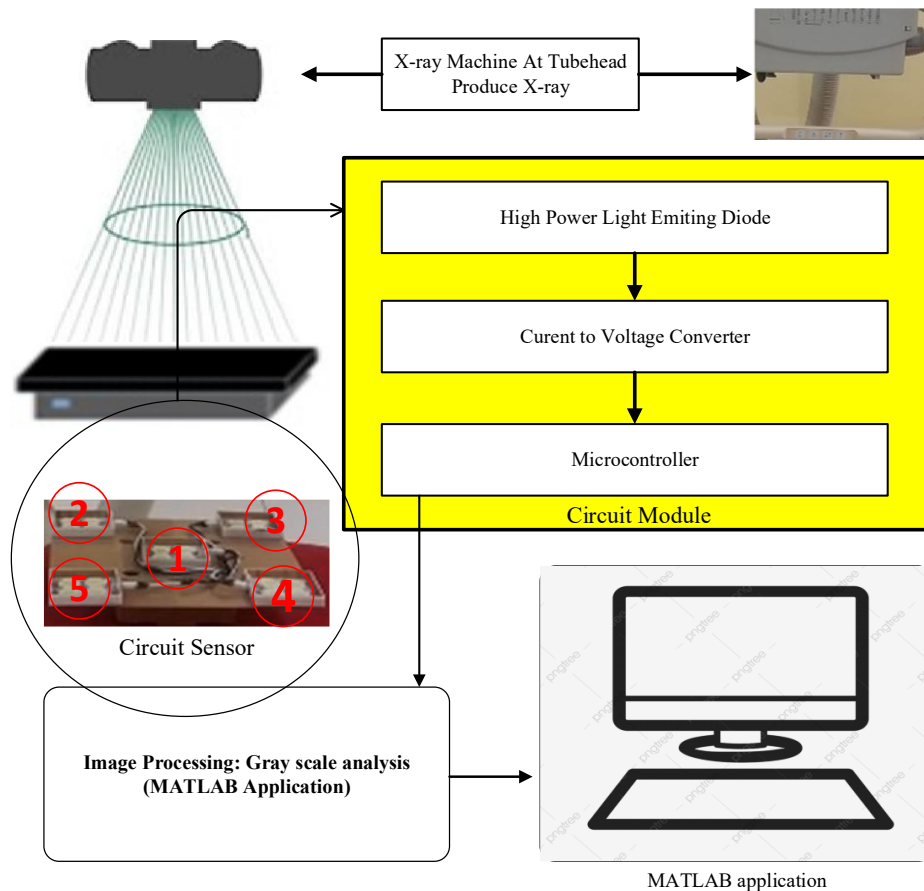


FIGURE 1. Shows a block diagram of this research system. A detector module that uses a high-power LED as a sensor, consisting of 5 sensor placement points, each sensor consisting of 4 LEDs that have a fluorescent phosphor coating. In this study, we only process data from the data in each corner, we call it S2, S3, S4, and S5. The LED receives X-rays from the tube head, generating an electric current. The converter circuit converts current into voltage as input to the microcontroller to be processed and sent to the PC via cable. An application is made on the PC to display the KV value of the x-rays emitted by the tube head.

points, see Figure 1 of the detector S2-S5. The collimation area was 20 cm square. The phosphor coating further converted the x-rays into visible light. Furthermore, this light was captured by the LED so that it can cause a voltage difference between the anode and cathode on the LED. Comparison was then carried out using the Fluke KV meter. The Philips U-Arm type digital x-ray radiography device was used as an experimental subject which further provided x-rays to the designed detector module and the Fluke Standard detector.

B. Methods

As a result of research in the manufacture of x-ray kV detectors, a comparison of the measurement results of the module with the x-ray equipment was carried out. Tools employed were PHILIP brand. Comparisons were conducted by comparing the measurement value of the tool module with the kV on x-rays. The test was carried out 3 times with data collected at 4 kV setting points, including 40kV, 50kV, 60kV, and 70kV. Based on this test, it will be known whether the measurement of the value produced by the module is following the standard as a reference point [36]–[38].

In the tool measurement stage, the module used a distance of 60 cm from the x-ray, using a setting of 1 second and also 80 mA. In data retrieval, each data had

a 5 minutes delay, which was intended to prevent damage to the x-ray plane. The sensor was placed at the end of the x-ray collimation with a distance of 20 cm x 20 cm. After this step was done, the result value was displayed on the PC using the application. The block diagram in this research system can be seen in Figure 1.

When the radiology machine provided an X-ray, the X-rays were captured by the LED and then processed in the microcontroller into data and sent to the PC application for further processing. The results were in the forms of numbers which further were displayed on a PC via the microcontroller and cable. A small box was provided under the X-ray field. It had 4 measurement points according to the collimation end, those are S2, S3, S4, and S5 measurement points. The module worked when the sensor was given x-rays. Furthermore, when the electric quantity was sensitive to the emission of X-ray photons, the sensor also acted as a semiconductor detector such as a photodiode. Those sensors had a direct energy band gap, also called converters in the sense that they convert energy from one form (photons) to another form (current). This is where the transducer output signal generated by radiation is in the form order to enter the Arduino which requires a voltage in the form of (V) then we use a circuit, namely current to voltage,

which converts current to volts so that it can be processed by Arduino and displayed to the application and processed in the form of numerical results.

Since each sensor produced different outputs, adjustments were needed in the Arduino by providing a multiplier as well as increasing and decreasing the reference so that all sensors will have the same reading value. After the sensor reading value was processed, the data were sent to the application via serial communication. The data read by application from serial communication, were further processed to find the peak value which were then converted into a unit value of kV. The kV value obtained then was displayed in the application.

III. Result

The module works when the detector is given x-rays. In this case, when the electric quantity is sensitive to the emission of X-ray photons, the detector also acts as a semiconductor detector such as a photodiode. Such detectors that have a direct energy band gap, also called converters in the sense that they convert energy from one form (photons) to another form (current). This is where the transducer output signal generated by the radiation (mV). In this case, to enter Arduino which requires a voltage (V), we used a circuit, namely current into voltage, which converted current into voltage so that it can be processed by Arduino and were displayed to the application and processed in the form of numerical results. The results obtained were explain as follow.

In the first experiment, we used the x-ray factor setting at 40 V, 80 mA, and 1 second time. After the data processing using a microcontroller and an application on a PC, the measurement results were obtained as presented in Table 1. Based on the measurement results using the tool module, the lowest value obtained was 30.25kV at the S4 measurement point, while the highest value obtained was 46kV at the S5 measurement point. It can be seen that the data were almost close to each measurement point, but were different between the measurement points. Furthermore, the smallest error was obtained in S2 by 0.83 percent, while the largest error obtained was in S4 by 13.75 percent.

TABLE 1

Data analysis results on X-Ray settings with 40 KV. The average value of each measurement point is quite different, especially in S4 as presented below.

NO	PARAMETER (kV)	STANDARD READING			
		T2	T3	T4	T5
1	Detector	40.25	40	30.25	46
2		40.25	36.25	36.5	38.75
3		38.5	40.5	36.75	36.5
Average		39.67	38.92	34.5	40.42
Std Deviation		0.82	1.90	3.01	4.05
%Error		0.83	2.71	13.75	-1.04
UA		0.48	1.10	1.74	2.34

Figure 2 below shows a graph depicting the results of measurement using kV 40 KV setting. The two measurement points of S2 and S3, show that the curve

is close to 40 and there is less change between each experiment. However, the other two measurement are actually slightly away from the number 40. In this case, S4 displays data below 40, while S5 exceeds 40.

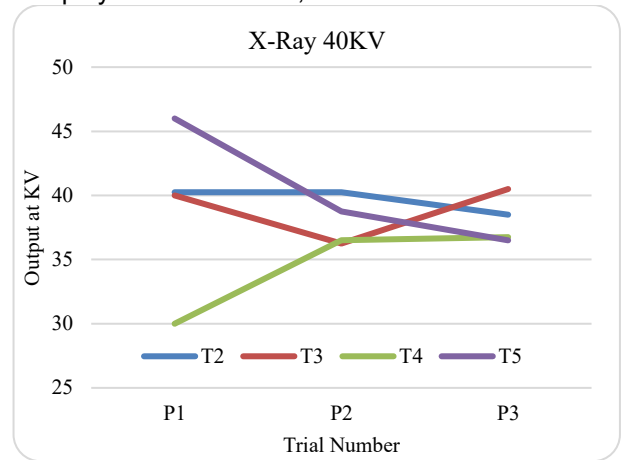


FIGURE 2 The curve above shows that the longer the experiment, the closer the setting value.

In the second experiment, we used the x-ray factor setting at 50 kV, 80 mA, and 1 second time. After the data processing using a microcontroller and an application on a PC, the measurement results were obtained and presented in Table 2. Based on the measurement results using the tool module, the lowest value obtained was 46.25kV at the S2 measurement point, while the highest value obtained was 63.25 kV at the S4 measurement point. It can be seen that the data were almost close to each measurement point, but were different between measurement points. In this case, the smallest error obtained was in S2 by 1.33 percent, while the largest error was obtained in S3 by 6 percent.

TABLE 2

Data analysis results on X-Ray settings with 50 KV. The measurement value on the first experiment looks much higher and the last one is close to the setting value

NO	PARAMETER (kV)	STANDARD READING			
		T2	T3	T4	T5
1	Detector	55	62.5	63.25	62.5
2		46.75	49	43	49
3		46.25	47.5	48.25	47.5
Average		49.33	53.00	51.50	53.00
Std Deviation		4.01	6.75	8.59	6.75
%Error		1.33	-6.00	-3.00	-6.00
UA		2.32	3.89	4.95	3.89

Figure 3 below shows a graph depicting the results of measurements made using the 50 KV setting. In the first experiment, it looks far beyond the setting, after that, the experiments 2 and 3 is far below the set value.

In the third experiment, we used the x-ray factor setting at the 60 kV, 80 mA, and 1 second time. After the data processing using a microcontroller and an application on a PC, the measurement results were obtained and presented in Table 3. As seen in table 3, based on the measurement results using the tool module, the lowest value was 40.25 kV at the S5 measurement point, while the highest value was 51.25 kV at the S3 measurement

point. It can be seen that the data were almost close to each measurement point, but were different between measurement points. In this case, the smallest error obtained was in S2 by 15 percent, while the largest error was obtained in S3 by 24.03 percent.

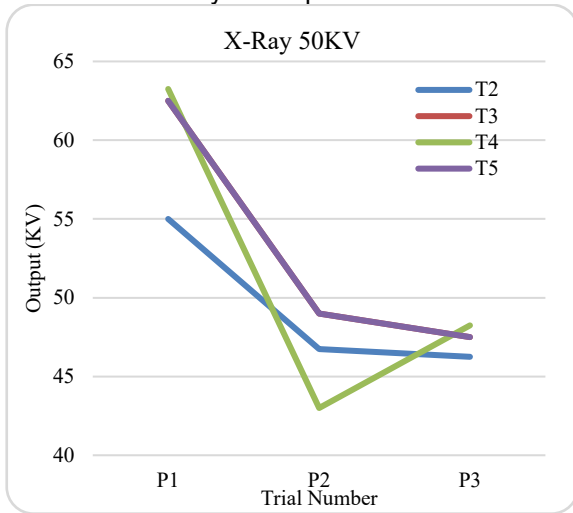


FIGURE 3 At setting 50 KV, the curve above shows that the longer the experiment, the closer to the setting value

TABLE 3

Data analysis results on X-Ray settings with 60 KV. The measurement value in this experiment is still far from being close to the setting value

NO	PARAMETER (kV)	STANDARD READING			
		T2	T3	T4	T5
1	Detector	51.25	50.5	50.5	40.25
2		51.25	48.25	47.5	48.25
3		50.5	51.25	49.5	48.25
Average		51.00	50.00	49.17	45.58
Std Deviation		0.35	1.27	1.25	3.77
%Error		15.00	16.67	18.06	24.03
UA		0.20	0.74	0.72	2.18

In the fourth experiment, the x-ray factor setting used was at 70 kV, 80 mA, and 1 second time. After the data processing using a microcontroller and an application on a PC, the measurement results were obtained and presented in Table 4. Based on the measurement results as presented in Table 4 using the tool module, the lowest value obtained was 40.75 kV at the S4 measurement point, while the highest value obtained was 61 kV at the S4 measurement point. It can be seen that the data were almost close to each measurement point, but were different between measurement points. In this case, the smallest error obtained was in S2 by 11.03 percent, while the largest error was obtained in S5 by 26.43 percent.

TABLE 4

Data analysis results on X-Ray settings with 60 KV. The measurement value in this experiment is still far from being close to the setting value

NO	PARAMETER (Kv)	STANDARD READING			
		T1	T2	T3	T4
1	Detector	61	57.25	58.75	59.5
2		50.5	52	50.5	54.25
3		54.25	53.5	55	40.75
Average		55.25	54.25	54.75	51.50
Std Deviation		4.34	2.21	3.37	7.90
%Error		21.07	22.50	21.79	26.43
UA		2.51	1.27	1.95	4.56

Eventually, it can be concluded from the tool module developed has shortcomings. The main finding of this research is that High-Power LEDs can be a detector for non-invasive measurement of X-ray KV meter, but in this research, the error is less stable and linear.

IV. Discussion

The results of the detector module under study were still much larger in error than the detectors from research using PMT with solar cell sensors and NaI (TI), [24], [28]. In this case, the drawback of the module that the author developed is that the problem with the detector itself which is less stable and linear. This may be solved by replacing the supporting circuit of the detector to get the desired value. The implications of the results of this study are the initial basis for the use of high-power sensors in non-invasive X-ray KV factor detection. The shortcoming of this study states the instability of the results can be reduced by several amplifier regression circuits. In addition, this study has limitations that make the error unstable and the data cannot be linear. This is due to the use of LEDs whose specifications have not been determined. The mechanism for converting x-rays into visible light also still used the phosphor features of non-standard LEDs. Additionally, the subject used was still one unit of x-ray machine. Therefore, it is expected that the next research will use several x-ray machines to obtain a better result.

V. Conclusion

The purpose of this study was to utilize high-power LED at a low-cost non-invasive x-ray KV meter detector design and test the ability of the detector at each point of collimation. Based on the results of the discussion and the purpose of developing the module, it can be concluded that a high power led tool can be utilized as a non-invasive kV meter detector in the field of irradiation collimation (tip). However, the results obtained from the detector itself are still less stable and linear. For the best result, the smallest error is at 40kV. In this case, the lowest error rate obtained is in S2 by 0.83%, while the highest error is obtained in S5 by 26.43%. The module results have a sufficiently large error, so it can be concluded that the detector can indeed detect x-rays, but the detector is not intended as a detector kV meter. For further research, the best quality LEDs can be used and research can be done on Analog Signal conditioners for the LEDs.

References

- [1] K. B. Lysdahl and B. M. Hofmann, "What causes increasing and unnecessary use of radiological investigations? a survey of radiologists' perceptions," BMC Health Serv. Res., vol. 9, pp. 1–9, 2009, DOI: 10.1186/1472-6963-9-155.
- [2] M. Bhargavan and J. H. Sunshine, "Utilization of radiology services in the United States: Levels and trends in modalities, regions, and populations," Radiology, vol. 234, no. 3, pp. 824–832, 2005, DOI: 10.1148/radiol.2343031536.
- [3] A. Matin, D. W. Bates, A. Sussman, P. Ros, R. Hanson, and R. Khorasani, "Inpatient radiology utilization: Trends over the past decade," Am. J. Roentgenol., vol. 186, no. 1, pp. 7–11, 2006, doi: 10.2214/AJR.04.0633.

- [4] S. Semin, Y. Demiral, and O. Dicle, "Trends in diagnostic imaging utilization in a university hospital in Turkey," *Int. J. Technol. Assess. Health Care*, vol. 22, no. 4, pp. 532–536, 2006, DOI: 10.1017/S0266462306051488.
- [5] S. Ketelhut, L. Büermann, and G. Hilgers, "Catalog of x-ray spectra of Mo-, Rh-, and W-anode-based x-ray tubes from 10 to 50 kV," *Phys. Med. Biol.*, vol. 66, no. 11, 2021, doi: 10.1088/1361-6560/abfbb2.
- [6] J. Ródenas, S. Gallardo, and M. C. Burgos, "Simulation models to obtain X-ray spectra using the Compton scattering technique," 2003 *Int. Conf. Phys. Control. PhysCon 2003 - Proc.*, vol. 1, pp. 228–231, 2003, DOI: 10.1109/PHYCON.2003.1236822.
- [7] I. Børretzen, K. B. Lysdahl, and H. M. Olerud, "Diagnostic radiology in Norway - Trends in examination frequency and collective effective dose," *Radiat. Prot. Dosimetry*, vol. 124, no. 4, pp. 339–347, 2007, DOI: 10.1093/rpd/ncm204.
- [8] A. Chrysanthopoulou et al., "Trends and future needs in clinical radiology: Insights from an academic medical center," *Health Policy (New York)*, vol. 80, no. 1, pp. 194–201, 2007, DOI: 10.1016/j.healthpol.2006.03.007.
- [9] C. S. Moore, T. J. Wood, A. W. Beavis, and J. R. Saunderson, "Correlation of the clinical and physical image quality in chest radiography for average adults with a computed radiography imaging system," *Br. J. Radiol.*, vol. 86, no. 1027, 2013, DOI: 10.1259/bjr.20130077.
- [10] C. Austerlitz, H. Mota, H. Gay, D. Campos, R. Allison, and C. Sibata, "On the need for quality assurance in superficial kilovoltage radiotherapy," *Radiat. Prot. Dosimetry*, vol. 130, no. 4, pp. 476–481, 2008, DOI: 10.1093/rpd/ncn067.
- [11] M. A. Mubarak, E. Yulianto, and T. B. Indrato, "Scintillation X-Ray Kv Meter," pp. 1–10, 2018.
- [12] C. M. Ma et al., "AAPM protocol for 40-300 kV x-ray beam dosimetry in radiotherapy and radiobiology," *Med. Phys.*, vol. 28, no. 6, pp. 868–893, 2001, DOI: 10.1118/1.1374247.
- [13] M. Ismail, M. Afzal, M. Nadeem, A. M. Rana, S. Amjad, and S. A. Buzdar, "Evaluation of depth dose characteristics of superficial X-rays machine using different KVP and applicators diameter," *Iran. J. Radiat. Res.*, vol. 9, no. 3, pp. 159–166, 2011.
- [14] Jorge Luis Domínguez Martínez, "Design of a Preamplifier Card for the Photomultiplier Tubes of a Gamma Camera," *J. Phys. Sci. Appl.*, vol. 8, no. 1, pp. 2–3, 2018, doi: 10.17265/2159-5348/2018.01.006.
- [15] W. Fu et al., "Development of an Ultra-Fast Photomultiplier Tube with Pulse-Dilation Technology," *IEEE Access*, vol. 8, pp. 47533–47537, 2020, DOI: 10.1109/ACCESS.2020.2979756.
- [16] C. D'Ambrosio, F. De Notaristefani, H. Leutz, D. Puertolas, and E. Rosso, "X-ray detection with a scintillating YAP-window hybrid photomultiplier tube," *IEEE Trans. Nucl. Sci.*, vol. 47, no. 1, pp. 6–12, 2000, doi: 10.1109/23.826891.
- [17] J. F. Briesmeister, "MCNPTM – A General Monte Carlo N-Particle Transport Code," *Los Alamos Natl. Lab.*, no. March, p. 790, 2000.
- [18] J. Ródenas, S. Gallardo, S. Ballester, V. Primault, and J. Ortiz, "Application of the Monte Carlo method to the analysis of measurement geometries for the calibration of an HPanGe detector in an environmental radioactivity laboratory," *Nucl. Instruments Methods Phys. Res. Sect. B Beam Interact. with Mater. Atoms*, vol. 263, no. 1 SPEC. ISS., pp. 144–148, 2007, DOI: 10.1016/j.nimb.2007.04.210.
- [19] J. Ródenas, A. Martinavarró, and V. Rius, "Validation of the MCNP code for the simulation of Ge-detector calibration," *Nucl. Instruments Methods Phys. Res. Sect. An AcAnel. Spectrometers, Detect. Assoc. Equip.*, vol. 450, no. 1, pp. 88–97, 2000, doi: 10.1016/S0168-9002(00)00253-9.
- [20] R. J. Tanner et al., "Intercomparison on the usage of computational codes in radiation dosimetry," *Radiat. Prot. Dosimetry*, vol. 110, no. 1–4, pp. 769–780, 2004, DOI: 10.1093/rpd/nch228.
- [21] L. Pan et al., "Acquiring and Modeling of Si Solar-Cell Transient Response to Pulsed X-Ray," *IEEE Trans. Nucl. Sci.*, vol. 68, no. 5, pp. 1152–1160, 2021, doi: 10.1109/TNS.2021.3067193.
- [22] C. Ossig et al., "X-ray beam induced current measurements for multi-modal x-ray microscopy of solar cells," *J. Vis. Exp.*, vol. 2019, no. 150, 2019, DOI: 10.3791/60001.
- [23] A. M. Crawford et al., "Development of a single-cell X-ray fluorescence flow cytometer," *J. Synchrotron Radiat.*, vol. 23, no. 4, pp. 901–908, 2016, DOI: 10.1107/S1600577516008006.
- [24] D. Meena and S. K. Gupta, "The Measurement of Efficiency and Resolution for CdZnTe and NaI (Ti) detectors," no. January 2019, pp. 1–2, 2021.
- [25] A. H. Ali, A. K. Mheemeeed, and H. I. Hassan, "Efficiency calibration study of NaI(TL) detector for radioactivity measurements in soils from Ain Zalah oil field," *World Appl. Sci. J.*, vol. 32, no. 3, pp. 359–367, 2014, doi: 10.5829/idosi.wasj.2014.32.03.955.
- [26] C. Davids, "Calibration of Pulse-Shape Discriminating NaI (Ti) Detectors," no. April 2016, 1989.
- [27] E. Barbosa de Souza et al., "Study of cosmogenic radionuclides in the COSINE-100 NaI(Tl) detectors," *Astropart. Phys.*, vol. 115, no. September, 2020, doi: 10.1016/j.astropartphys.2019.102390.
- [28] N. YAVUZKANAT, S. YALÇIN, and D. Güngör, "The Determination of the Total Efficiency for NaI(Tl) Detector by GATE Simulation," *Bitlis Eren Üniversitesi Fen Bilim. Derg.*, vol. 8, no. May 2021, pp. 37–45, 2019, doi: 10.17798/bitlisfen.649129.
- [29] A. S. H. . T. M. T. . B. Y. M., "Study the Factors Affecting the Quality Assurance of Superficial Radiotherapy X-Ray Machine," *Int. J. Sci. Res.*, vol. 4, no. 4, pp. 1316–1319, 2015.
- [30] P. A. Evans, A. J. Moloney, and P. J. Mountford, "Performance assessment of the Gulmay D3300 kilovoltage X-ray therapy unit," *Br. J. Radiol.*, vol. 74, no. 882, pp. 537–547, 2001, DOI: 10.1259/bjr.74.882.740537.
- [31] M. S. Patterson, "Photodynamic therapy dosimetry: A TO Z," no. 88. 2016. DOI: 10.1142/9789814719650_0008.
- [32] M. C. Schell et al., "Stereotactic Radiosurgery Report of Task Group 42 Radiation Therapy Committee for the American Association of," no. 5, p. 50, 1995.
- [33] E. Damulira, M. N. S. Yusoff, A. F. Omar, N. H. Mohd Taib, and N. M. Ahmed, "Application of Bpw34 photodiode and cold white LED as diagnostic X-ray detectors: A comparative analysis," *Appl. Radiat. Isot.*, vol. 170, no. February, p. 109622, 2021, DOI: 10.1016/j.apradiso.2021.109622.
- [34] R. Santoso, D. Titisari, P. ATP, H. Gumiwang Ariswati, and L. Lamidi, "Evaluating of a Super Bright LED As a Spectrophotometer Light Source at The Clinical Laboratory," *J. Electron. Electromed. Eng. Med. Informatics*, vol. 4, no. 1, pp. 24–34, 2022, DOI: 10.35882/jeeemi.v4i1.3.
- [35] E. Damulira, M. N. S. Yusoff, A. F. Omar, and N. H. M. Taib, "Amplification of radiation-induced signal of the LED strip by an increasing number of LED chips and using amplifier board," *Appl. Sci.*, vol. 10, no. 2, 2020, DOI: 10.3390/app10020651.
- [36] C. Of, S. Practice, F. O. R. The, and U. S. E. Of, "Code of Safe Practice for the Use of," no. June. 2010.
- [37] R. Azzoz, K. M. ElShahat, and R. A. MonemRezk, "Evaluation of Quality control systems for X-Ray machines at different Hospitals using patient's radiological dose assessment technology," *IOSR J. Appl. Phys.*, vol. 6, no. 5, pp. 29–34, 2014, DOI: 10.9790/4861-06512934.
- [38] D. R. Ningtias, S. Suryono, and S. Susilo, "Pengukuran Kualitas Citra Digital Computed Radiography Menggunakan Program Pengolah Citra," *J. Pendidik. Fis. Indones.*, vol. 12, no. 2, pp. 161–168, 2016, doi: 10.15294/jpfi.v12i2.5950.